Hadroproduction of photons and leptons

F. Halzen and D. M. Scott
Physics Department, University of Wisconsin, Madison, Wisconsin 53706
(Received 17 April 1978)

We calculate the spectrum of lepton pairs produced in hadronic collisions to first order in α_s in quantum chromodynamics (QCD). We compare the results with the data and identify further experimental tests. We emphasize that the same QCD graphs which generate the transverse momentum of lepton pairs also yield real photons at high transverse momentum, and calculate the resulting cross sections.

I. INTRODUCTION

The study of scaling violations in deep-inelastic leptoproduction has become the outstanding experimental probe of the underlying quark-gluon dynamics [quantum chromodynamics (QCD)] of hadrons.[1] These analyses are unfortunately obscured by the choice of scaling variable, the production of heavy quarks (e.g., charm) giving scaling violations because of their thresholds, which are fixed in the total energy, and possible mass scale effects due to the mass of the weak intermediate boson(s), especially in the case of ν-induced interactions. Our major goal in this paper[2] is to identify clean experimental tests of QCD in the hadroproduction of virtual[3,4] and real photons[2] which are not obscured by these or similar problems. We show how these data provide an alternative testing ground for perturbative QCD. The phenomenological advantage relies on the fact that the effects of quark-gluon dynamics cannot only be observed through modulation on the (scaling) cross section but directly confronted with the transverse-momentum distributions of the produced virtual photon. Although the production of leptons and photons in hadronic collisions produces a wealth of information which can be directly and unambiguously compared with QCD calculations, our formal theoretical understanding falls unfortunately short of that achieved with regard to lepton-induced interactions.[5]

The bremsstrahlung of gluons by quarks introduces scaling violations into the structure function describing the longitudinal-momentum distribution $F(x)$ of quarks inside hadrons. It also gives a transverse-momentum component to the previously longitudinal motion of the quarks. These effects can be computed[6] in the lowest order of the quark-gluon coupling constant α_s and are observable as scaling violations in the structure function $F(x, Q^2)$, where Q^2 is the momentum transfer of the virtual-photon probe. In the Drell-Yan picture[7] of the production of lepton pairs by quark-antiquark annihilation [Fig. 1(a)] the gluon-bremsstrahlung effects are observable through the transverse motion of the quarks, resulting in the transverse momentum of the virtual photon. In an alternative picture, the transverse motion of the virtual photon can originate from quark-antiquark annihilation into a photon-gluon pair [Fig. 1(b)] or from the Compton scattering of quarks and gluons [Fig. 1(c)]. Scaling violations in the Drell-Yan process can therefore be computed from (i) the pair annihilation and Compton scattering of quarks and gluons [Figs. 1(b) and 1(c)], or (ii) the scaling violations in the quark structure functions. Politzer[3] has shown to order α_s that one can actually choose the scale Q_0 of the theory in such a way that both pictures (i) and (ii) lead to identical scaling violations in the lepton-pair cross section (integrated over their transverse momentum). This is pictorially represented in Fig. 2(a). The two pictures are complementary, double counting would result if one were to add the

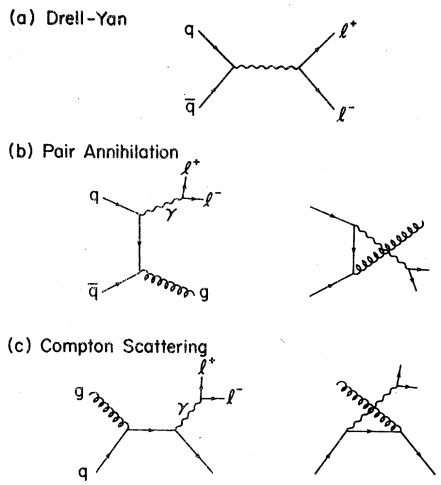

FIG. 1. The hadroproduction of lepton pairs in lowest-order QCD: (a) Drell-Yan mechanism; (b) quark-antiquark annihilation into a photon and a gluon; (c) "Compton" scattering of quark-gluon into quark-virtual photon. In this and the following figures, curly (wiggly) lines represent gluons (photons).

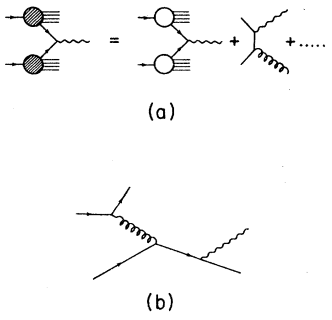

FIG. 2. (a) Politzer's theorem—the shaded (open) blobs represent structure functions which have (do not have) QCD scaling violations in $O(\alpha_s)$; (b) an $O(\alpha_s{}^2)$ diagram, which is important because it involves quarks from both incident hadrons.

two mechanisms, i.e., Fig. 1 with QCD-corrected structure functions, and the diagrams of Figs. 1(b) and 1(c). We will present a simple derivation of Politzer's theorem for the quark-gluon mechanism in Sec. II. The problem of investigating the interplay of (i) and (ii) at fixed p_T has not been solved and is further obscured by the unfortunate situation that higher-order diagrams in α_s cannot be ignored, e.g., the diagram of Fig. 2(b). Schematically, the diagrams of Figs. 1(b) and 1(c) can be written as $(\alpha_s Q\bar{Q} + \alpha_s QG)$, where Q ($\bar{Q}$) and G represent quark (antiquark) and gluon hadron structure functions. The diagram of Fig. 2(b) is of the type $\alpha_s{}^2 QQ$ and competes with the lower-order diagrams because of the suppression of antiquarks and gluons in the present kinematical regime. If one absorbs the upper quark-gluon vertex in the QCD-corrected structure function, the diagram of Fig. 2(b) reduces to a Compton diagram of Fig. 1, and this again puts into focus the unsolved question of the possible addition of mechanisms (i) and (ii) at fixed p_T.

In this paper we investigate a "minimal" model: In the lowest order we calculate the four diagrams of Figs. 1(b) and 1(c) combined with scaling structure functions. As Politzer's theorem has not been proven at fixed p_T, this might be an incomplete estimate of QCD effects; it certainly constitutes a lower-bound calculation. Given this, we try to identify straightforward tests of the model, devoid of the type of unavoidable problems we mentioned in connection with scaling violations in leptoproduction. Phenomenological confrontation of QCD with hadroproduction data of leptons can be plagued by the following:

(a) Infrared divergence of the diagrams of Figs. 1(b) and 1(c). Massless quarks and gluons can scatter with zero-momentum transfer where the diagrams of Figs. 1(b) and 1(c) diverge. In QED, finite masses push this divergence outside the physical region due to the "$t_{\min}$ effect." The divergence can be controlled by introducing arbitrarily effective quark and gluon masses, or a transverse-momentum cutoff.

(b) Confinement effects. Quarks and gluons inside hadrons have some "internal" transverse motion,[8] which is associated, e.g., with the 300-MeV transverse-momentum cutoff of π secondaries in hadron collisions. These effects contribute of course to the (small) p_T behavior of produced leptons and therefore to $\langle p_T \rangle$ values.

The celebrated test of computing the $\langle p_T \rangle$ of a produced lepton pair as a function of its invariant mass suffers from both above-mentioned deficiencies. We argue that QCD calculations should be confronted instead with the (large) p_T dependence of the lepton-pair cross section at fixed invariant mass m. Despite the fact that the minimal model contains no free parameters, the data from Fermilab[9] can be successfully accommodated. We show that measurements of the energy and rapidity dependence of this quantity as well as its variation with a change of beam-particle type could provide us with further tests of the perturbative QCD calculations.

We especially emphasize the fact that the same QCD mechanism that generates the transverse momentum of virtual photons yields real photons[10] at large p_T. The underlying assumption of QCD that one can use perturbation theory in the quark-gluon coupling constant in the impulse approximation (large momentum transfer Q, high energy) regardless of the space-like or timelike nature of Q allows us to apply the diagrams of Figs. 1(b) and 1(c) to the production of real photons at large p_T. The argument is schematically represented in Fig. 3. The expansion in α_s is valid because of the large momentum flow in the quark-gluon diagram. It is now sustained by the transverse momentum of the produced photon instead of the mass of the lepton pair. The assumptions are identical to those made in QCD calculations of

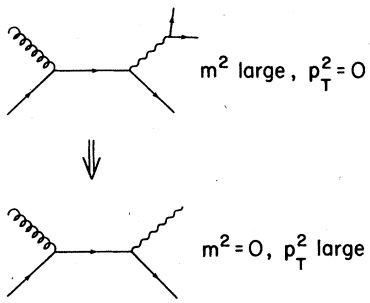

FIG. 3. Schematic representation of the argument that the same QCD graphs relevant to the hadroproduction of lepton pairs yield large-p_T direct photons.

the hadronic production of secondary hadrons with high transverse momentum.[11] We predict production of direct photons very close to present experimental limits[12] in pp collisions. γ/π^0 ratios at the 10% level are obtained for $p_T = 4-6$ GeV, with $(pp \to \pi X) \simeq (pp \to \gamma X)$ at $p_T \simeq 10$ GeV. We investigate in detail the relative merit of π, $\bar{p}$, and p beams in the production of direct photons as well as the p_T and energy dependence of the cross sections.

We describe in Sec. II A the details of the calculation and reserve Sec. II B for its phenomenological confrontation with the data. Direct photon production is discussed in Sec. III. We conclude in Sec. IV with some closing remarks regarding the production of weak intermediate bosons and the problem of quark transverse momenta in high-p_T phenomena.

II. THE MINIMAL MODEL

A. Calculation of diagrams: Politzer's theorem, an illustration

In this section we will introduce the formalism, and illustrate Politzer's theorem as an example of how to apply it. In the next subsection we will present the phenomenology and compare the QCD calculations to the data. The relevant QCD subprocesses—pair annihilation and Compton scattering—have been previously described and are shown in Figs. 1(b) and 1(c). The full cross section to this order in α_s is obtained by calculating the diagram of Fig. 4, where momenta are defined. B, T, and SP labels stand for beam, target, and subprocess, respectively. We take the beam and target, as well as quarks and gluons, to be massless. We define

$$\begin{aligned} s &= 2a\cdot b\,, \\ t &= (a-p)^2 = -2a\cdot p + m^2\,, \\ u &= (b-p)^2 = -2b\cdot p + m^2\,. \end{aligned} \tag{2.1}$$

Here we introduce the usual notation for the four-momentum p of the virtual photon, with $p^2 = m^2$. The subprocess invariants are denoted by primed variables and are

$$\begin{aligned} s' &= x_1 x_2 s\,, \\ t' &= x_1 t + (1-x_1)m^2\,, \\ u' &= x_2 u + (1-x_2)m^2\,. \end{aligned} \tag{2.2}$$

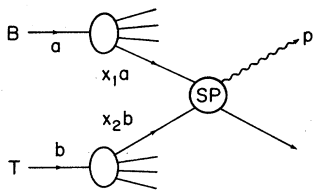

FIG. 4. Structure of QCD diagrams for the hadroproduction of lepton pairs. B, T, and SP refer respectively to beam, target, and subprocess.

The invariant cross section for the subprocess is

$$\frac{E d\sigma}{dm^2 d^3p} = \frac{s'}{\pi}\frac{d\sigma}{dm^2 dt'}\delta(s'+t'+u'-m^2)\,, \tag{2.3}$$

from which we calculate the $O(\alpha_s)$ hadronic cross section to be

$$E\frac{d\sigma}{dm^2 d^3p} = \int dx_1 dx_2 f^B(x_1) f^T(x_2)\frac{s'}{\pi} \times \frac{d\sigma}{dm^2 dt'}(s',t',u')\delta((x_1 a + x_2 b - p)^2)\,. \tag{2.4}$$

f^B and f^T are the appropriate longitudinal-momentum distribution functions for the constituents carrying momenta $x_1 a$ and $x_2 b$. Using the δ function to eliminate the x_2 integration, Eq. (2.4) reduces to

$$E\frac{d\sigma}{dm^2 d^3p} = \frac{s}{\pi}\int_{x_1^{\min}}^{1} dx_1 f^B(x_1) f^T(x_2)\frac{x_1 x_2}{x_1 s + u - m^2} \times \frac{d\sigma}{dm^2 dt'}(s',t',u')\,, \tag{2.5}$$

with

$$x_2 = \frac{-x_1 t - (1-x_1)m^2}{x_1 s + u - m^2} \tag{2.6}$$

and

$$x_1^{\min} = \frac{-u}{s+t-m^2}\,. \tag{2.7}$$

In order to reduce the expression for the invariant cross section of Eq. (2.5) to the usual momentum variables y (center-of-mass rapidity) and p_T (transverse momentum) of the virtual photon, we note the following transformations:

$$\frac{d\sigma}{dy dp_T{}^2} = \pi E\frac{d\sigma}{d^3p} \tag{2.8}$$

and

$$\begin{aligned} t &= -s^{1/2} m_T e^{-y} + m^2\,, \\ u &= -s^{1/2} m_T e^{y} + m^2\,, \end{aligned} \tag{2.9}$$

where m_T is the transverse mass

$$m_T{}^2 = m^2 + p_T{}^2\,. \tag{2.10}$$

The diagrams of Fig. 1 are now simply computed by substituting $d\sigma/dm^2 dt$ of the relevant subprocesses into Eq. (2.5). They are given by

(i) Drell-Yan [Fig. 1(a)]

$$\frac{d\sigma}{dm^2dt} = \frac{4\pi\alpha^2}{3s}\delta(m^2-s)\delta(t), \tag{2.11}$$

(ii) pair annihilation [Fig. 1(b)]

$$\frac{d\sigma}{dm^2dt} = \frac{8\alpha^2\alpha_s}{27m^2}\frac{(t-m^2)^2+(u-m^2)^2}{s^2tu}, \tag{2.12}$$

(iii) Compton scattering [Fig. 1(c)]

$$\frac{d\sigma}{dm^2dt} = \frac{\alpha^2\alpha_s}{9m^2}\frac{s^2+u^2+2m^2t}{-s^3u}. \tag{2.13}$$

These cross sections must be weighted by the relevant squared quark charge. We take the running coupling constant α_s varying with m^2 in the sense of asymptotic freedom, although none of our results are sensitive to this variation. The cross sections of Eqs. (2.11), (2.12), and (2.13) are obtained from the QED cross sections for producing virtual photons of mass m^2 by "sticking" on the leptons through a multiplicative factor $\alpha/(3\pi m^2)$ and by introducing the appropriate color factors. These are respectively given in terms of the λ matrices of the SU(3) color group by

$$\text{(i) } \tfrac{1}{3}, \quad \text{(ii) } \tfrac{1}{9}\sum_a \mathrm{Tr}\tfrac{1}{2}\lambda^a\tfrac{1}{2}\lambda^a = \tfrac{4}{9},$$

$$\text{(iii) } \tfrac{1}{24}\sum_a \mathrm{Tr}\tfrac{1}{2}\lambda^a\tfrac{1}{2}\lambda^a = \tfrac{1}{6}.$$

As an illustration of the formalism, we present a derivation of Politzer's theorem for the Compton scattering subprocess. We perform the calculation for $p_T^2 \to 0$ at fixed y and m^2. We note that

$$\begin{aligned}
&t \to -(sm^2)^{1/2}e^{-y}+m^2,\\
&u \to -(sm^2)^{1/2}e^{y}+m^2,\\
&x_1^{\min} \to \tau^{1/2}e^{y},\\
&x_2 \to \tau^{1/2}e^{-y},\\
&x_1 s+u-m^2 \to s(x_1-\tau^{1/2}e^{y}),\\
&u' = -x_1 s p_T^2/(x_1 s+u-m^2),\\
&s'^2+u'^2+2m^2t' \to x_1^2x_2^2s^2[(1-\tau_{12})^2+\tau_{12}^2],
\end{aligned} \tag{2.14}$$

where $\tau_{12}=\tau/x_1x_2$ and $\tau=m^2/s$. From this and Eqs. (2.5), (2.8), and (2.13) we find that

$$\frac{d\sigma}{dm^2dydp_T^2} \to \frac{4\pi\alpha^2}{9m^2sp_T^2}\frac{\alpha_s}{2\pi}\int_{\tau^{1/2}e^{y}}^1 \frac{dx_1}{x_1}G^B(x_1) \times \frac{F_2^T(x_2)}{x_2}\frac{(1-\tau_{12})^2+\tau_{12}^2}{2}, \tag{2.15}$$

with $x_2=\tau^{1/2}e^{-y}$. G^B is the longitudinal-momentum distribution of a gluon in the beam, and F_2^T is the electromagnetic structure function of the target.

After integration over p_T^2, with a suitable cutoff to avoid the divergence, we obtain to leading logarithms

$$\frac{d\sigma}{dm^2dy} = \frac{4\pi\alpha^2}{9m^2s}\frac{\alpha_s}{2\pi}\ln\frac{m^2}{\mu^2}\int_{\tau^{1/2}e^{y}}^1 \frac{dx_1}{x_1}G^B(x_1) \times \frac{F_2^T(x_2)}{x_2}\frac{(1-\tau_{12})^2+\tau_{12}^2}{2}. \tag{2.16}$$

The scaling parton-model Drell-Yan formula is given by Eqs. (2.5), (2.8), and (2.11),

$$\frac{d\sigma}{dm^2dy} = \frac{4\pi\alpha^2}{9m^2s}\sum_i e_i^2 q_i^B(x_1)q_{\bar{i}}^T(x_2), \tag{2.17}$$

with $x_1=\tau^{1/2}e^{y}$, $x_2=\tau^{1/2}e^{-y}$. This is also the QCD formula to lowest (zeroth) order in α_s in this context. We note that comparison of Eqs. (2.16) and (2.17) leads to the replacement

$$q_i^B(x) \to q_i^B(x) + \frac{\alpha_s}{2\pi}\ln\frac{m^2}{\mu^2}\int_x^1 \frac{dy}{y}G^B(y)\frac{1}{2}\left[\left(1-\frac{x}{y}\right)^2+\left(\frac{x}{y}\right)^2\right], \tag{2.18}$$

which is the same as the corresponding first-order corrections to quark and antiquark distributions in electroproduction.[6] For the pair annihilation diagrams this procedure would not give the complete answer, since wave functions and vertex corrections also exist[3] in the same order in α_s.

B. Explicit computation of the minimal model: Phenomenology

We now compute explicitly the minimal model combining the diagrams of Fig. 1 with *scaling* quark (and gluon) distributions. Indeed, as we are calculating the numerator to first order in α_s, scaling violations to the cross section appearing in the denominator of

$$\langle p_T^2\rangle = \left(\int dp_T^2 p_T^2 \frac{d}{dm^2dydp_T^2}\right)\Big/\frac{d\sigma}{dm^2dy} \tag{2.19}$$

formally contribute to $O(\alpha_s^2)$ to $\langle p_T^2\rangle$. Since the numerator is $O(\alpha_s)$, they should not be included. The quark distributions are then completely determined by leptoproduction data and the measured cross sections[9] $d\sigma/dmdy$ at $y=0$ via Eq. (2.17). We assume an SU(3)-symmetric sea, and obtain[13]

$$\begin{aligned}
u_v(x) &= 2.99(1-x)^4(1+5.99x-2.63x^{1/2})x^{-1/2},\\
d_v(x) &= 1.02(1-x)^5(1+5.75x)x^{-1/2},\\
s(x) &= 0.44(1-x)^9x^{-1}(0.8760+3.087x-4.408x^2\\
&\qquad -74.07x^3+209.9x^4-102.3x^5).
\end{aligned} \tag{2.20}$$

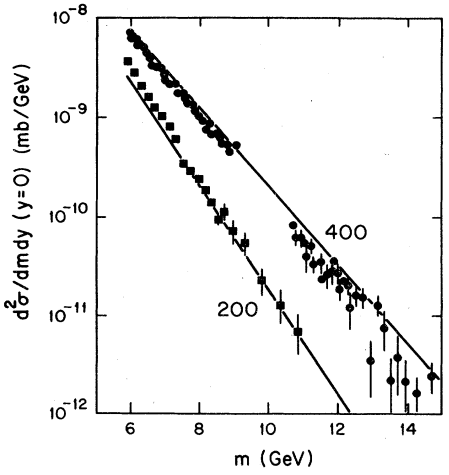

FIG. 5. The cross section (Ref. 9) for the production of lepton pairs in proton-nucleus collisions is plotted along with the parton-model calculation using the structure functions of Eq. (2.20).

The cross section reconstructed from these distributions is shown in Fig. 5. We also note that extrapolations of the distributions of Eq. (2.20) outside the currently measured kinematic region are at best uncertain. When calculating π-induced interactions, we take for the quark distributions[14] in a π

$$u_v^\pi = 0.54(1-x)^{2.55}(1+7.9x)x^{-1/2}, \qquad s^\pi = 0.1(1-x)^5 x^{-1}. \tag{2.21}$$

Gluon distributions are fixed by assuming that the gluons carry approximately half the hadron momentum and by dimensional counting.[15] This results in the momentum distributions

$$G^P(x) = 3(1-x)^5/x, \tag{2.22}$$

so that indeed

$$\int_0^1 xG^P(x)dx = 0.5 \tag{2.23}$$

and

$$G^\pi(x) = 2(1-x)^3/x, \tag{2.24}$$

so that again

$$\int_0^1 xG^\pi(x)dx = 0.5. \tag{2.25}$$

We will try to identify features of the calculation that do not crucially depend on the quark structure functions, and to this extent dimensional counting of gluon fractional momenta is the only assumption beyond QCD. The calculation is free of parameters: Absolute normalizations as well as the momentum dependence of the cross sections are fixed in the minimal model once the structure functions are chosen. We now proceed to evaluate (i) average transverse momenta, (ii) transverse-momentum dependence of the inclusive lepton-pair cross section.

We will show that at large p_T, where comparison with the data is reliable, quark-gluon Compton scattering dominates the pp calculation. The quark-antiquark annihilation graph, on the contrary, dominates πp and $\bar{p}p$ interactions. Therefore, *sea-quark* (as opposed to valence) *distributions do not affect any qualitative features of our calculations*, although they have been consistently included in the computations.

1. $\langle p_T \rangle$ and $\langle p_T^2 \rangle$

We calculate $\langle p_T^2 \rangle$ as a function of the mass of the lepton pair, and the rapidity,[16] using Eq. (2.19). For the numerator we use our QCD calculation outlined in the previous subsection. Although the cross section itself diverges as $p_T^2 \to 0$, the result is integrable for all four diagrams when multiplied by p_T^2 to form the numerator of Eq. (2.19). The cross sections corresponding to the graphs of Figs. 1(b) and 1(c) diverge as $(1/p_T^2)\ln p_T^2$ and $1/p_T^2$, respectively. So for $\langle p_T^2 \rangle$, the infrared divergence causes no calculational problems. However, the p_T moment is still weighted by the divergent unphysical small-p_T cross section, as will become obvious from subsequent calculations. In Fig. 6 we show the result by plotting $\langle p_T^2 \rangle$ at

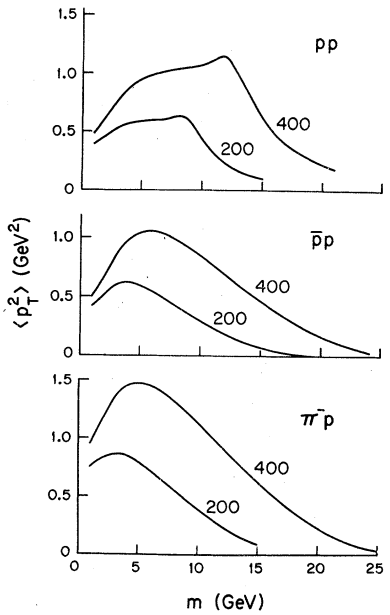

FIG. 6. The average squared transverse momentum of lepton pairs produced in hadronic interactions, calculated from QCD.

$y=0$ for pp, $\bar{p}p$, and $\pi^- p$ collisions, at laboratory momenta 200 and 400 GeV. Note the sharp drop in $\langle p_T \rangle$ for large lepton-pair masses in $\pi^- p$ and $\bar{p}p$ collisions compared to pp interactions, where the average transverse momentum is quasi m^2 independent up to the phase-space cutoff. This is a relic of the steeper angular dependence of the pair annihilation diagrams which dominate in $\pi^- p$ and $\bar{p}p$ interactions, as compared to Compton scattering which dominates in the pp case.

The results can be nicely summarized by writing $\langle p_T{}^2 \rangle$ in its "scaling" form; on purely dimensional grounds we can write that (see also Altarelli *et al.* in Ref. 4)

$$\langle p_T{}^2 \rangle = \alpha_s s F(\tau, \alpha_s, y) . \tag{2.26}$$

In the order of perturbation theory in which we are working, F has no α_s dependence—this develops in higher orders. In Fig. 7 we show our calculation of F at $y=0$ for pp, $\bar{p}p$ and $\pi^- p$ collisions. We note that near the kinematic upper limits for $p_T{}^2$ and τ our results depend crucially on the parametrization of Eq. (2.20), that is, the perturbation expansion may become unreliable.

What is shown in Figs. 6 and 7 is the result of the QCD calculation, which here cannot be compared directly with the data, because the internal transverse momentum of the interacting constituents (quarks and gluons) has to be taken into account. It is this "Fermi motion" of the quarks and gluons confined to hadrons that one observes indirectly in the 300-MeV transverse-momentum cutoff of diffraction scattering. Little is known about it theoretically,[17] for example, whether it is s or x dependent. As it has to be added to the QCD calculation in order to make any comparison to the data possible, it is clear that much of the predictive power is stripped from the calculation of $\langle p_T \rangle$ or $\langle p_T{}^2 \rangle$. To make an illustrative calculation of $\langle p_T \rangle$ in pp collisions, we make the strong

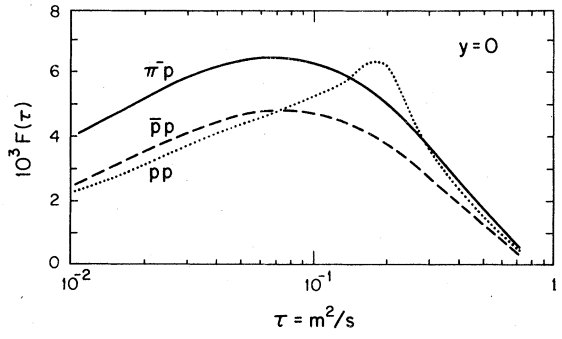

FIG. 7. The value of the function $F(\tau, y)$, which gives the average squared transverse momentum of lepton pairs via Eq. (2.26), $\langle p_T{}^2 \rangle = \alpha_s s F(\tau, y)$, is plotted versus $\tau = m^2/s$ at $y=0$.

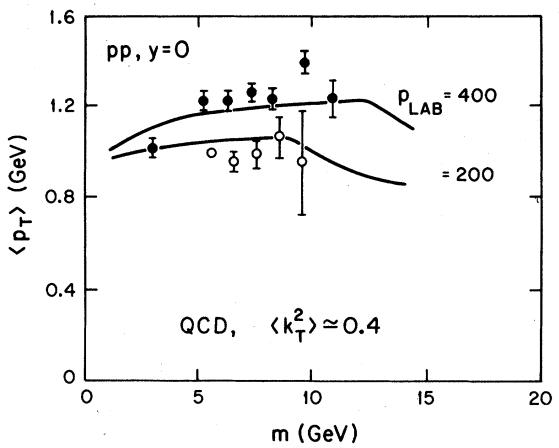

FIG. 8. The average transverse momentum of lepton pairs produced in pp collisions has been calculated [see Eq. (2.26)] from the QCD diagrams of Figs. 1(b) and 1(c), assuming an intrinsic transverse momentum of quarks and gluons to be $\langle k_T{}^2 \rangle = 0.4$ GeV^2. The data are from Ref. 9.

assumption that the quarks' and gluons' internal squared transverse momentum is constant, and take it to be 0.4 GeV^2. We then calculate $\langle p_T \rangle$ by

$$\langle p_T \rangle \simeq \left[\frac{\pi}{4}\left(2\times 0.4 + \langle p_T{}^2 \rangle\right)\right]^{1/2}, \tag{2.27}$$

assuming approximately Gaussian distributions. The result is shown in Fig. 8 for two incident laboratory momenta, 200 and 400 GeV, where there are data.[9] The procedure we have outlined gives both the magnitude and energy dependence of the $\langle p_T \rangle$ data, but we emphasize that this result relies strongly on our assumption about the internal quark transverse momentum. Moreover, the calculation is unreliable for small values of m^2. The observed decrease of $\langle p_T \rangle$ for $m^2 < m_\psi{}^2$ is expected from the universal scaling of strong-interaction processes in transverse mass[2,18] and has, most likely, no relevance to QCD calculations.

So far we have presented results for $y=0$. We now proceed to discuss the Feynman $x_F = 2P_L/\sqrt{s}$ predictions of the calculation. In Fig. 9 we plot $\langle p_T{}^2 \rangle$ versus x_F for a lepton-pair mass of 9 GeV, at $p_{\rm lab} = 400$ GeV. The pp and $\bar{p}p$ curves are symmetric of course about $x_F = 0$, and it turns out that the $\pi^- p$ curve is very nearly symmetric. Remember that here too the internal quark momentum must be added before the results can be compared to data. By studying the x_F behavior of Eq. (2.15), one can show that

$$\frac{d\sigma}{dm^2 dy dp_T{}^2} \propto (x_F^{\max} - x_F)^{n_q} \tag{2.28}$$

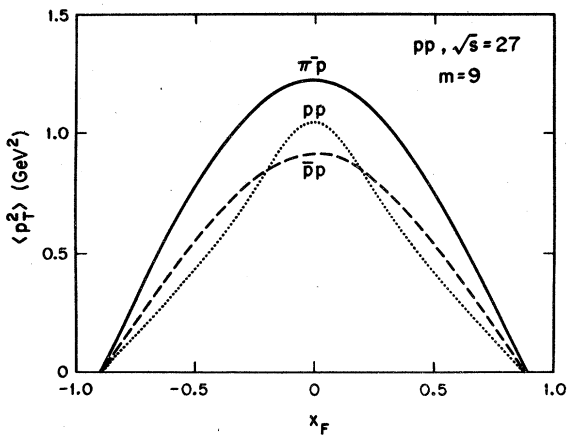

FIG. 9. The Feynman-x_F dependence of the average squared transverse momentum of lepton pairs of mass 9 GeV produced in hadronic collisions at $\sqrt{s}=27.4$ GeV.

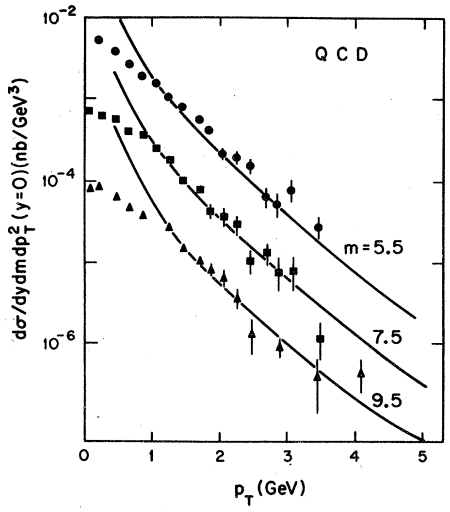

FIG. 10. The transverse-momentum spectrum of lepton pairs produced in pp collisions at $y=0$, at $\sqrt{s}=27.4$ GeV, for $m=5.5$, 7.5, and 9.5 GeV. The curves show the QCD calculation from Eq. (2.5). The data are from Ref. 9. One should keep in mind that normalization of the data has a 40% systematic error (Ref. 9).

as $x_F \to x_F^{\max} = (1-\tau)$. Here n_q is defined by

$$q(x) \underset{x\to 1}{\longrightarrow} (1-x)^{n_q} . \tag{2.29}$$

Equations (2.19) and (2.28) yield

$$\langle p_T{}^2 \rangle \propto (x_F^{\max} - x) . \tag{2.30}$$

This behavior is consistent with the full computation shown in Fig. 9 and essentially results from kinematics; as $x_F \to x_F^{\max}$, phase space requires that $p_T{}^2 \propto (x_F^{\max} - x)$, yielding Eq. (2.30).

Although the above results are suggestive and encouraging, additional assumptions make the phenomenology unreliable. Because of the theoretical problems related to its computation (infrared divergences and internal k_T) we do not consider $\langle p_T{}^2 \rangle$ measurements to be reliable test of QCD. The main value of their measurement in the present context resides in the fact that the discrepancy between QCD $\langle p_T{}^2 \rangle$ moments and data gives us a hint as to the magnitude and possible kinematic dependence of the internal k_T. This is valuable information in a completely different theoretical context.[8] We now proceed to discuss how to obtain a direct test of the theory.

2. $d\sigma/dm^2 dy dp_T{}^2$

Consider the transverse-momentum spectrum of the lepton pairs. At sufficiently high transverse momentum we can, hopefully, neglect the limited, internal transverse momentum of the quarks. This is what provides us with a direct test of the calculation—the high-p_T spectrum depends on just its two main ingredients: (i) the fractional longitudinal-momentum distributions, and (ii) the QCD subprocess dynamics.

Data taken in a proton beam at $p_{\text{lab}} = 400$ GeV and $y=0$ are shown in Fig. 10 for three values of the lepton-pair mass, along with our calculation. For $p_T > 1$–2 GeV it gives a good description of the data; for small values of p_T any comparison with data is of course meaningless because of the divergence of $p_T \to 0$ discussed in Sec. II A. At higher p_T the results are unaffected by any cutoff to avoid the divergence and the agreement between data and calculation is therefore significant. In Fig. 11(a) we show the breakdown of the transverse-momentum distribution according to its two sources: pair annihilation and Compton scattering. For $p_T \gtrsim 1$ GeV the Compton scattering dominates, in fact, by as much as an order of magnitude at $\langle p_T \rangle \simeq 4$ GeV. The result does not depend on the detailed form of the sea Eq. (2.20). *The high-transverse-momentum lepton-pair spectrum is a direct manifestation of gluon dynamics.*

We have checked that this qualitative agreement is not sensitive to (i) explicit inclusion of internal k_T with $\langle k_T \rangle$ of order 1 GeV; (ii) nuclear corrections for the target; (iii) inclusion of scaling violations in the structure functions; (iv) the detailed structure of gluon-momentum distributions. We illustrate the latter in Fig. 11(b), where the effect is shown for a change from $n_g = 5$ to 7 in the $(1-x)^{n_g}$ behavior of the gluon structure function.

A further test is provided by the energy dependence of the high-p_T spectrum. The spectra at 200 and 400 GeV for lepton-pair masses 5.5 and 7.5 GeV are shown in Fig. 12. In Fig. 13 we show the beam-particle dependence of these spectra.

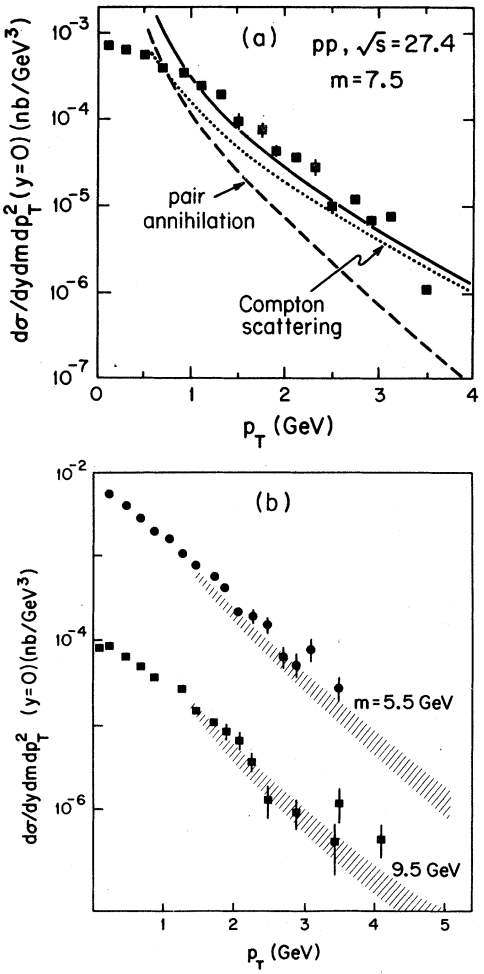

FIG. 11. (a) The QCD calculation for the transverse-momentum spectrum of lepton pairs with mass 7.5 GeV produced in pp collisions at $y=0$ and $\sqrt{s}=27.4$ GeV is shown separated into its two components, quark-antiquark annihilation, and quark-gluon Compton scattering. (b) The QCD calculation for the transverse-momentum spectrum of lepton pairs with mass $m=5.5$ and 9.5 GeV produced in pp collisions at $y=0$ and $\sqrt{s}=27.4$ GeV is shown for a range of gluon structure functions $(1-x)^{n_g}$, with $n_g=5$–7 and normalization form Eq. (2.23).

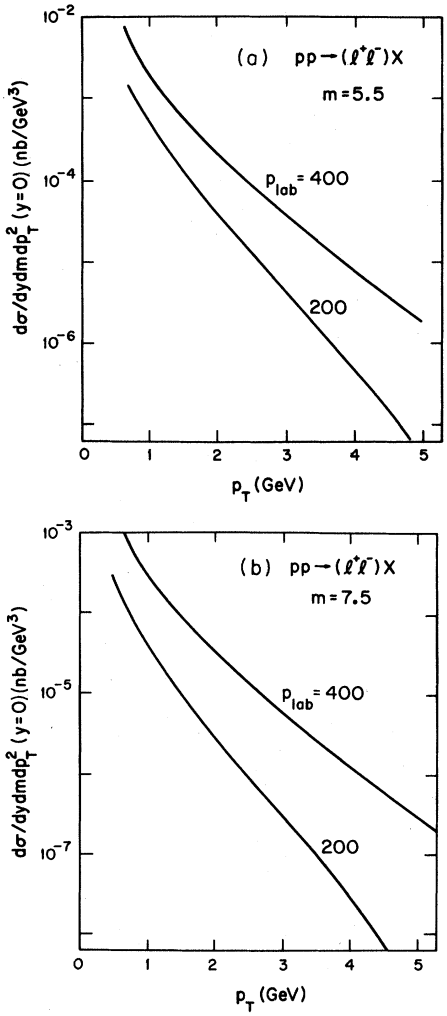

FIG. 12. The energy dependence of the transverse-momentum spectrum of lepton pairs produced in pp collisions at $y=0$. (a) $m=5.5$ GeV; (b) $m=7.5$ GeV.

In $\bar{p}p$ and $\pi^- p$ collisions, it is the pair annihilation contribution which dominates, as valence-valence annihilations are available. Finally, Figs. 14 and 15 illustrate the trends of the Feynman-x_F dependence of $d\sigma/dx_F dm dp_T{}^2$ in pp and $\pi^- p$ interactions, respectively. In each case we computed the x_F dependence of the lepton-pair cross section at fixed p_T, as well as the p_T dependence at fixed values of x_F.

Note that the $x_F \to x_F^{\max}$ limit at large p_T is simply determined by the large-x_F behavior of the structure functions. The argument is similar to counting rules in high-p_T processes; we obtain, for example,

$$E\frac{d\sigma}{dm^2 d^3p} \propto (x_F^{\max}-x)^{n_q+n_g+1} \tag{2.31}$$

for the dominant quark-gluon graph in pp collisions.

III. REAL PHOTONS

We pointed out in the Introduction that the same QCD diagrams which produce the transverse momentum of massive virtual photons completely determine the production of real photons at high transverse momentum. The formalism developed in the previous section applies; we remove the leptons with a factor $3\pi m^2/\alpha$, and then set $m^2=0$. We used the same quark and gluon distributions

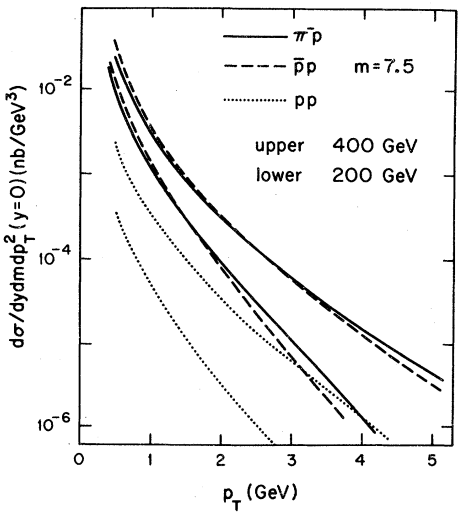

FIG. 13. The beam-particle dependence of the transverse-momentum spectrum of lepton pairs at $y=0$ with $m=7.5$ GeV.

as for the lepton-pair calculation. For high-p_T photons produced in pp collisions, the form of the sea is irrelevant, since the photons come dominantly from quark-gluon scattering. For $\pi^- p$ and $\bar{p}p$, valence-valence annihilations dominate, and so the form of the sea is again unimportant.

Our results for direct photon production in pp collisions at $y=0$ and at various energies are shown in Fig. 16. The ratios of the production by different beam-particle types are shown in Fig. 17. At high x_T the production of $\pi^- p$ and $\bar{p}p$ collisions is enhanced relative to pp by the availability of valence-valence annihilations. For small x_T the ratios depend on the detailed size of the quark sea in the nucleon; we therefore expect Fig. 17 to give at best a qualitative description of the ratios when $x_T \simeq 0$.

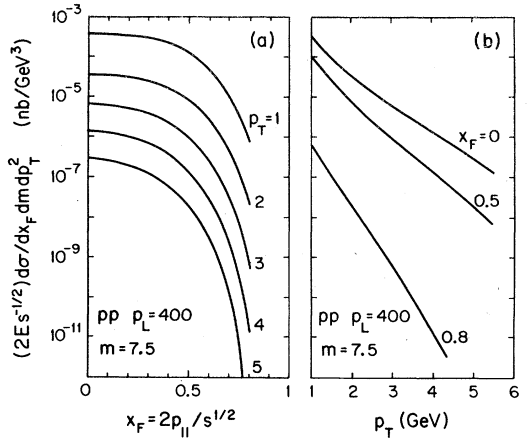

FIG. 14. The Feynman-x_F dependence of the transverse-momentum spectrum of lepton pairs of mass 7.5 GeV produced in pp collisions at $\sqrt{s}=27$ GeV. Shown is (a) the x_F dependence at fixed representative values of p_T and (b) the p_T dependence at fixed representative value of x_F.

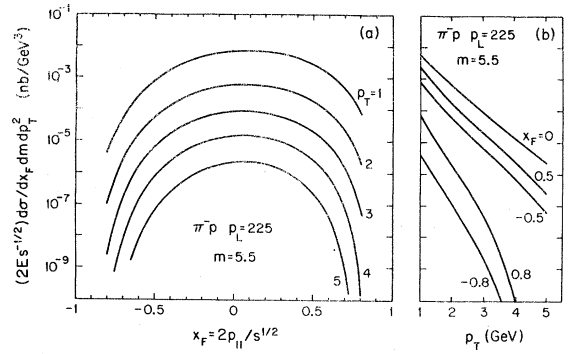

FIG. 15. Same as Fig. 14 for $\pi^- p$ collisions.

In Fig. 18 we show the direct photon yield in pp collisions as a function of p_T at $p_{\text{lab}}=400$ GeV. We have plotted the experimentally relevant ratio

$$\frac{\gamma}{\pi^0} \equiv \frac{Ed^3\sigma/dp^3(Ap \to \gamma X)}{Ed^3\sigma/dp^3(Ap \to \pi^0 X)}$$

at $y=0$. We divide the calculated photon cross sections by a QCD calculation[11] for production of large-p_T π's. We only show the calculation for p_T values where the π calculation has been confirmed by data (see also Fig. 19). The γ/π ratio is a prediction of our photon calculation independent of the validity of the π QCD calculation, to the extent that it successfully interpolates the data in the kinematic range shown in Fig. 18. We also repeated the pp calculation for $\sqrt{s}=63$ GeV.

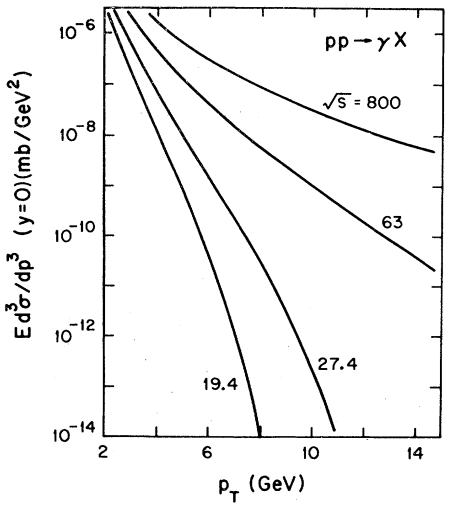

FIG. 16. The cross section for the production of direct photons at high p_T in pp collisions, calculated from QCD.

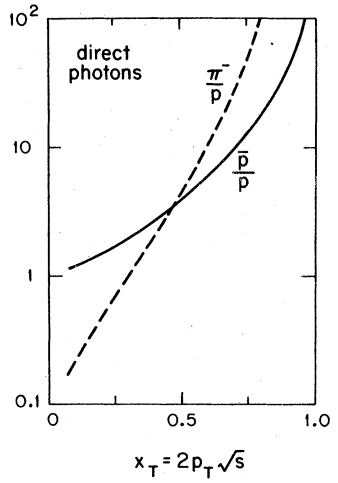

FIG. 17. Ratios of yield of direct photons in $\pi^- p$ and $\bar{p}p$ collisions to that in pp collisions.

In Fig. 19 we directly compare data[20] as well as our QCD calculation for the $pp \to \pi^0 X$ inclusive cross section at $y = 0$ and $\sqrt{s} = 53$ GeV with the computed direct photon yield. This clearly shows $\gamma/\pi^0 \simeq 10\%$ for $p_T \simeq 4$–6 GeV and $\gamma/\pi^0 \simeq 1$ for $p_T \simeq 10 \sim 15$ GeV.

It might be thought that the γ/π^0 ratio would be enhanced by increasing the energy to, say $\sqrt{s} = 400$–800 GeV. This is not so, because at these energies QCD mechanisms are relevant for hadronic production at high p_T, too,[11] and γ/π^0 stays relatively small. So perhaps the best place to see

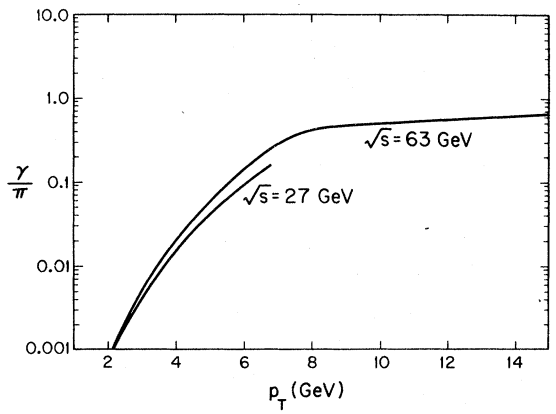

FIG. 18. Direct photon yield in pp collisions. Plotted is

$$\gamma/\pi^0 = \frac{Ed\sigma/d^3p\,(Ap \to \gamma X)}{Ed\sigma/d^3p\,(Ap \to \pi^0 X)}$$

at $x_F = 0$ and $\sqrt{s} = 27$, 63 GeV. Numerator and demoninator are calculated in QCD (see Ref. 11 for π^0 calculation.) In the p_T ranges shown, the QCD π^0 cross section interpolates existing data (Refs. 19 and 20).

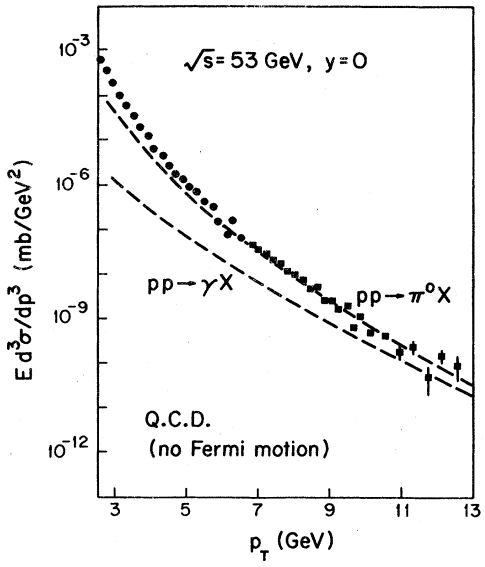

FIG. 19. Cross sections for high-p_T γ's and π^0's, at 90° and $\sqrt{s} = 53$ GeV calculated from QCD. Fermi motion has not been included in the π^0 calculation shown (Ref. 11 and 21). Also shown are π^0 data from Ref. 20.

the direct photons is at very high transverse momentum at Fermilab and ISR energies.

IV. DISCUSSION AND CLOSING REMARKS

Confrontation of $\langle p_T \rangle$ measurements of lepton pairs with QCD perturbative results to order α_s is encouraging. A detailed comparison of the theory and the data is, however, impossible because of our ignorance regarding the "internal" transverse momentum of quarks and gluons. In order to account for existing data, the average squared transverse momentum of a quark must be rather large, $\langle k_T^2 \rangle_{\text{quark}} \simeq 0.4$–$0.5$ GeV^2 compared to $\langle k_T^2 \rangle \simeq 0.15$ GeV^2 for π secondaries in hadrons. Of course, quarks are expected to carry a larger transverse momentum than the hadrons into which they materialize. However, the s, Bjorken-x, and parent-particle dependence of this quantity is completely unknown. Unless one knows the internal $\langle k_T^2 \rangle$, QCD is stripped of any predictive power regarding this quantity.

We subsequently showed that the same problems do not exist for the lepton-pair cross section at large transverse momentum, where the quark or gluon internal transverse momentum is negligible compared to the transverse momentum generated in the hard subprocess, pair annihilation, or Compton scattering. The large-p_T spectrum of direct leptons in all its detail, m dependence, s dependence, y dependence, and beam-particle dependence should provide a strong test of QCD

ideas.

We emphasize that the direct-photon test must be passed at the same time; to order α_s in QCD the mechanism producing high-p_T lepton pairs is the same mechanism that produces high-p_T real photons. The calculated rates are large; QCD predicts the experimental observation of direct photons.

The question obviously arises as to why not go beyond the minimal model? The simple answer is that the theoretical problem has not been solved. There are no renormalization-group equations here which can be invoked to give the result of summing all orders in perturbation theory, as there are for leptoproduction. We presented the phenomenology of these $O(\alpha_s)$ calculations with the hope that the perturbation expansion is relevant; comparison with existing data suggests that it is. Furthermore, the experimental situation calls for a phenomenological attack of the problem:

(i) Data already exist for which our analysis is relevant, and soon much more data on lepton-pair production and direct photons should appear.

(ii) The hunt for the W and Z^0 (in singular or plural) is coming close. Knowledge of the transverse-momentum spectra of heavy bosons is needed to help with their detection. Consider hadroproduction of a W at a typical hadron collider energy $\sqrt{s}=400$ GeV. The transverse momentum of the W will be given through conserved vector current (CVC) by Eq. (2.26), with F given approximately by Fig. 7. For $M_W=60$ GeV, $\tau=M_W^2/s=0.02$ so that $F\simeq 3\times 10^{-3}$. This means that, depending on the choice of α_s,

$$\langle p_T^2\rangle_W \simeq 50\text{–}80\ \text{GeV}^2 . \tag{4.1}$$

So the transverse momentum of a W is of the order of 10% of its mass at these energies. The consequent smearing of the lepton spectrum coming from the decay $W\to\mu\nu$ will make finding the W more difficult.

(iii) Quark transverse momenta have become the crucial link between QCD calculations and existing data on the hadroproduction of high-transverse-momentum hadrons.[21]

Our final remark concerns both QCD and the parton model. It is now widely believed that the cross section for the hadroproduction of lepton pairs integrated over transverse momentum depends on just the structure functions—quark densities—obtained from leptoproduction experiments. This relationship must constitute a very important test of QCD and the parton model. The data of Ref. 9 suggest that one may need a much bigger quark-antiquark sea to fit the lepton-pair data than one would normally contemplate in fitting leptoproduction. A possible origin for such an enhanced sea (given that we wish to retain color) is the mechanism proposed by Bjorken and Weisberg[22]—the sea is enhanced by the quarks and antiquarks from particles produced in the central region. Clearly, this mechanism is outside present QCD calculations, and its presence would require *different* sea parametrizations for the phenomenology of leptoproduction and lepton-pair production.

ACKNOWLEDGMENTS

This work was supported in part by the University of Wisconsin Research Committee with funds granted by the Wisconsin Alumni Research Foundation, and in part by the Energy Research and Development Administration under Contract No. EY-76-C-02-0881, COO-881-21.

[1] C. H. Llewellyn Smith, in *Proceedings of the 1975 International Symposium on Lepton and Photon Interactions at High Energies, Stanford, California,* edited by W. T. Kirk (SLAC, Stanford, 1976); L. Hand and O. Nachtmann, in *Proceedings of the International Symposium on Lepton and Photon Interactions at High Energies, Hamburg, 1977,* edited by F. Gotbrod (DESY, Hamburg, 1977).

[2] Our results have been briefly reported in F. Halzen and D. M. Scott, Phys. Rev. Lett. 40, 1117 (1978).

[3] H. D. Politzer, Nucl. Phys. B129, 301 (1977); see also C. T. Sachrajda, Phys. Lett. 73B, 185 (1978).

[4] J. Kogut, Phys. Lett. 65B, 377 (1976); I. Hichliffe and C. H. Llewellyn Smith, *ibid.* 65B, 281 (1977); J. C. Polkinghorne, Nucl. Phys. B116, 347 (1976); A. V. Radynshkin, Phys. Lett. 69B, 245 (1977); J. Kogut, and J. Shigemitsu, Cornell report (unpublished); K. Kajantie and R. Raitio, Helsinki Report No. HU-TFT-77-21 (unpublished); G. Altarelli, G. Parisi, and R. Petronzio, CERN Report No. TH. 2413 (unpublished); H. Fritzsch and P. Minkowski, Phys. Lett. 73B, 80 (1978); K. H. Craig and C. H. Llewellyn Smith, *ibid.* 72B, 349 (1978); K. Kajantie, J. Lindfors, and R. Raitio, *ibid.* 74B, 38 (1978); H. Georgi, Phys. Rev. D 17, 3010 (1978).

[5] H. D. Politzer, Phys. Rep. 14, 129 (1974).

[6] G. Altarelli and G. Parisi, Nucl. Phys. B126, 298 (1977).

[7] S. D. Drell and T.-M. Yan, Phys. Rev. Lett. 25, 316 (1970).

[8] Minh Duong-van, SLAC Report No. SLAC-PUB-1819 (unpublished); P. V. Landshoff, Phys. Lett. 66B, 452 (1977); J. F. Gunion, UC-Davis Report No. UCD-76-8 (unpublished); F. E. Close, F. Halzen, and D. M.

Scott, Phys. Lett. 68B, 447 (1977); A. C. Davis and E. J. Squires, Phys. Lett. 69B, 249 (1977); S. Matsuda, Rutherford Laboratory Report No. RL-77-068/A (unpublished); J. C. Polkinghorne, CERN Report (unpublished); R. J. Hughes, J. Phys. G 3, 255 (1977); M. Gronau and Y. Zarmi, Phys. Rev. D 18, 2341 (1978); J. S. Bell and A. J. G. Hey, CERN report (unpublished); J. Kripfganz and G. Ranft, CERN Report No. TH. 2398 (unpublished); C. Michael, Prog. Part. Nucl. Phys. (to be published); C. S. Lam and T.-M. Yan, Cornell report (unpublished); K. J. Kim, Phys. Lett. 73B, 45 (1978); J. Gunion and D. Soper, ibid. 73B, 189 (1978); R. C. Hwa, S. Matsuda, and R. G. Roberts, CERN Report No. Th 2456 (unpublished).

[9]S. W. Herb *et al.*, Phys. Rev. Lett. 39, 252 (1977); W. Innes *et al.*, *ibid.* 39, 1240 (1977); L. M. Lederman, in *Proceedings of the International Symposium on Lepton and Photon Interactions at High Energies, Hamburg, 1977*, edited by F. Gotbrod (DESY, Hamburg, 1977); Ben Lee Memorial International Conference, Fermilab, 1977 (unpublished); D. M. Kaplan *et al.*, Phys. Rev. Lett. 40, 435 (1978); K. J. Anderson *et al.*, *ibid.* 37, 799 (1976); R. Kephart, Vanderbilt Conference, Nashville, 1978 (unpublished).

[10]Recent calculations of direct photons include: G. R. Farrar, Phys. Lett. 67B, 357 (1977); F. Halzen, Rutherford Report No. RL-77-049/A (unpublished); H. Fritzsch and P. Minkowski, Phys. Lett. 69B, 316 (1977); S. Brodsky, private communication. See also C. O. Escobar, Nucl. Phys. B98, 173 (1975); Phys. Rev. D 15, 355 (1977); G. R. Farrar and S. C. Frautschi, Phys. Rev. Lett. 36, 1017 (1976).

[11]B. L. Combridge, J. Kripfganz, and J. Ranft, Phys. Lett. 70B, 234 (1977); R. Cutler and D. Sivers, Phys. Rev. D 16, 679 (1977); A. P. Contogouris (private communication); J. F. Owens, E. Reya, and M. Gluck, Phys. Rev. D 18, 1501 (1978); R. D. Field, Phys. Rev. Lett. 40, 997 (1978) and references therein.

[12]K. T. McDonald *et al.*, in *Proceedings of the International Conference on Production of Particles with New Quantum Numbers*, edited by D. B. Cline and J. J. Kolonko (University of Wisconsin, Madison, 1976); P. Darriulat *et al.*, Nucl. Phys. B (to be published).

[13]The valence distributions are taken from F. T. Dao, E. Flaminio, Kwan-Wu Lai, W. Metcalf, and Ling-Lie Wang, BNL report (unpublished). The sea is then chosen to fit the data of Ref. 9.

[14]R. D. Field and R. P. Feynman, Phys. Rev. D 15, 997 (1978); and Ref. 13.

[15]S. J. Brodsky and G. R. Farrar, Phys. Rev. Lett. 31, 1153 (1973); V. Matveev, R. Muradyna, and A. Tavkhelidze, Lett. Nuovo Cimento 7, 719 (1973).

[16]See also the work of Kajantie and Raitio, Ref. 4.

[17]See the wide variety of opinions in Ref. 8.

[18]F. E. Close and D. M. Scott, Phys. Lett. 69B, 173 (1977); C. Michael, Prog. Part. Nucl. Phys. (to be published).

[19]G. Donaldson *et al.*, Phys. Rev. Lett. 36, 1110 (1976).

[20]F. W. Busser *et al.*, Nucl. Phys. B106, 1 (1976); B. G. Pope in *Particles and Fields—1977*, Proceedings of the Meeting of the APS Division of Particles and Fields, Argonne, Illinois, edited by P. A. Schreiner, G. H. Thomas, and A. B. Wicklund (AIP, New York, 1978).

[21]F. Halzen, G. A. Ringland, and R. G. Roberts, Phys. Rev. Lett. 40, 991 (1978).

[22]J. D. Bjorken and H. Weisberg, Phys. Rev. D 13, 1405 (1976).